Title

Yellow fever disease severity and endothelial dysfunction are associated with elevated serum levels of viral NS1 protein and syndecan-1.

Authors

de Sousa, Francielle

Warnes, Colin

Manuli, Erika

et al.

Publication Date

2024-11-01

DOI

10.1016/j.ebiom.2024.105409

Peer reviewed

Yellow fever disease severity and endothelial dysfunction are associated with elevated serum levels of viral NS1 protein and syndecan-1

Francielle T. G. de Sousa,[a,b,c] Colin M. Warnes,[a] Erika R. Manuli,[b,c] Laurentia V. Tjang,[a] Pedro H. Carneiro,[a] Luzia Maria de Oliveira Pinto,[a,d] Arash Ng,[e] Samhita Bhat,[a] Jose Victor Zambrana,[f] Luiz G. F. A. B. D'Elia Zanella,[g] Yeh-Li Ho,[g] Camila M. Romano,[b,c] P. Robert Beatty,[a,e] Scott B. Biering,[a] Esper G. Kallas,[b,c,g] Ester C. Sabino,[b,c,*] and Eva Harris[a,e,**]

[a]Division of Infectious Diseases and Vaccinology, School of Public Health, University of California, Berkeley, Berkeley, CA 94720-3370, USA
[b]Departamento de Doenças Infecciosas e Parasitárias, Instituto de Medicina Tropical, Faculdade de Medicina da Universidade de São Paulo, São Paulo, SP 05403000, Brazil
[c]Laboratório de Investigação Médica, Hospital das Clínicas da Faculdade de Medicina da Universidade de São Paulo (HCFMUSP), São Paulo, SP 05403000, Brazil
[d]Laboratório das Interações Vírus-Hospedeiros (LIVH), Instituto Oswaldo Cruz, Fundação Oswaldo Cruz (IOC/Fiocruz), Rio de Janeiro 21040-360, Brazil
[e]Division of Immunology and Molecular Medicine, Department of Molecular and Cell Biology, University of California, Berkeley, Berkeley, CA, 94720-3200, USA
[f]Department of Epidemiology, School of Public Health, University of Michigan, Ann Arbor, MI, 48109, USA
[g]Hospital das Clínicas da Faculdade de Medicina da Universidade de São Paulo (HCFMUSP), São Paulo, SP 05403000, Brazil

eBioMedicine
2024;109: 105409
Published Online xxx
https://doi.org/10.1016/j.ebiom.2024.105409

Summary

Background Yellow fever virus (YFV) infections are a major global disease concern with high mortality in humans, and as such it is critical to identify clinical correlates of disease severity. While nonstructural protein 1 (NS1) of the related dengue virus is implicated in contributing to vascular leak, little is known about the role of YFV NS1 in severe YF and mechanisms of vascular dysfunction in YFV infections.

Methods Using serum samples from laboratory-confirmed YF patients with severe (n = 39) or non-severe (n = 18) disease in a well-defined hospital observational cohort in Brazil, plus samples from healthy uninfected controls (n = 11), we investigated factors associated with disease severity and endothelial dysfunction.

Findings We found significantly increased levels of NS1, as well as syndecan-1, a marker of vascular leak, in serum from severe YF as compared to non-severe YF or control groups. We also showed that hyperpermeability of endothelial cell monolayers treated with serum from severe YF patients was significantly higher compared to non-severe YF and control groups, as measured by transendothelial electrical resistance (TEER). Further, we demonstrated that YFV NS1 induces shedding of syndecan-1 from the surface of human endothelial cells. Notably, YFV NS1 serum levels significantly correlated with syndecan-1 serum levels, TEER values, and signs of disease severity. Syndecan-1 levels also significantly correlated with clinical laboratory parameters of disease severity, viral load, hospitalization, and death.

Interpretation This study provides further evidence for endothelial dysfunction as a mechanism of YF pathogenesis in humans and suggests serum quantification of YFV NS1 and syndecan-1 as valuable tools for disease diagnosis and/or prognosis.

Funding This work was supported by the US NIH and FAPESP.

*Corresponding author. Departamento de Doenças Infecciosas e Parasitárias, Instituto de Medicina Tropical, Faculdade de Medicina da Universidade de São Paulo, São Paulo, SP 05403000, Brazil.
**Corresponding author. Division of Infectious Diseases and Vaccinology, School of Public Health, University of California, Berkeley, Berkeley, CA 94720-3370, USA.
E-mail addresses: sabinoec@usp.br (E.C. Sabino), eharris@berkeley.edu (E. Harris), francielletg@gmail.com (F.T.G. de Sousa), pedrocarneiro@berkeley.edu (P.H. Carneiro), lpinto@ioc.fiocruz.br (L. Maria de Oliveira Pinto), arashng@berkeley.edu (A. Ng), josviczammad@gmail.com (J.V. Zambrana), ho.yeh@hc.fm.usp.br (Y.-L. Ho), cmromano@usp.br (C.M. Romano), prbeatty@berkeley.edu (P.R. Beatty), esper.kallas@usp.br (E.G. Kallas).

Keywords: Yellow fever; Pathogenesis; Endothelial dysfunction; NS1; Syndecan-1

Research in context

Evidence before this study

Yellow fever (YF) is a mosquito-borne systemic illness caused by yellow fever virus (YFV), a member of the *Flavivirus* genus. The disease can cause severe manifestations, including hepatic injury, endothelial damage, coagulopathy, hemorrhage, systemic organ failure, and shock, associated with high mortality in humans. YF pathogenesis is complex, and there is a limited number of studies focusing on the mechanism of endothelial impairment. Previous work from our group has shown that YFV nonstructural protein 1 (NS1) alone can induce endothelial disruption *in vitro* and vascular leak in mouse liver, and the mechanism was determined to include disruption of the endothelial glycocalyx. We searched the PubMed database several times from inception up until August 18, 2024, using the terms: "yellow fever" AND "endothelial" OR "vascular". Together, previous studies of YF in humans have described structural changes in the vascular milieu, immune cell infiltrates, and dysregulated hepatic and serum levels of proinflammatory and coagulation markers indicating cytokine storm and coagulopathy as important clinical findings. One article showed *in vitro* infection of endothelial cells by YFV and increased secretion of proinflammatory markers such as IL-6 and RANTES, suggesting that infection could contribute to endothelial activation. Endothelial damage was described mainly in the liver, but also in the heart, central nervous system, and lungs. In a study using serum from YF patients of the same studied cohort, angiopoietin 2, a serum biomarker of endothelial activation, was associated with mortality. While the literature shows evidence of endothelial impairment during YF, no results were found discussing YFV NS1 and syndecan-1 as possible correlates of disease severity.

Added value of this study

Using clinical samples from our hospital cohort in Brazil, we demonstrate that YF disease severity is associated with increased serum levels of the secreted viral protein NS1 and syndecan-1, a marker of vascular leak. We also find that YFV NS1 induces shedding of syndecan-1 from the surface of human endothelial cells *in vitro*. The data shown herein corroborate the involvement of YFV NS1 in endothelial dysfunction in YF patients, consistent with our previous findings *in vitro* and in mouse models. Together, our data supports that YFV NS1 and endothelial dysfunction are important components of YF pathogenesis. Further, we developed a YFV NS1 capture ELISA that serves as a proof-of-concept for low-cost NS1-based diagnosis/prognosis tools for YF.

Implications of all the available evidence

Despite the existing vaccine, outbreaks of human yellow fever can have disruptive effects on health care systems, with high hospitalization and mortality rates. In endemic regions, especially in underserved areas, YF is underreported, and symptomatic cases can be difficult to differentiate from other diseases such as malaria, leptospirosis, arenaviral diseases, viral hepatitis, and dengue. Our data introduce two new potential biomarkers (YFV NS1 and syndecan-1) as valuable tools that may help identify high-risk patients. This study also highlights the possibility of using affordable YFV NS1 detection assays for differential diagnosis in low-income countries.

Introduction

Yellow fever virus (YFV) is an arbovirus endemic to tropical areas of Central and South America and sub-Saharan Africa and is the causative agent of yellow fever (YF) disease. YF is considered a reemerging disease, with increasing infections over the past 20 years, exemplified by epidemics in 2015 and 2016 in Angola and the Democratic Republic of Congo and in 2016–2019 in Brazil.[1,2] The clinical spectrum of YF in humans ranges from asymptomatic infection to mild illness to severe disease. Manifestations of severe disease include vasculopathy and organ impairment of the liver, kidneys, lungs, intestine, and brain, resulting in high case fatality rates (20–60%).[2]

YFV is a member of the *Flavivirus* genus of the *Flaviviridae* family, with a positive-sense RNA genome of approximately 11 kb that encodes three structural and seven nonstructural proteins.[3] The *Flavivirus* nonstructural protein 1 (NS1) is secreted by infected cells and has been used as a serological diagnostic marker for dengue.[4] Further, dengue virus (DENV) NS1 levels have been correlated with disease severity.[5–7] We have shown that *Flavivirus* NS1 can directly cause vascular leak *in vitro* and in animal models in a tissue-specific manner that reflects viral disease tropism.[8,9] Mechanisms of NS1-induced endothelial dysfunction include disruption of key components of endothelial integrity such as the glycocalyx[8] and intercellular junctional complexes.[9,10] Further, studies have demonstrated that soluble *Flavivirus* NS1, independently from the virus, can act on endothelial cells to facilitate viral dissemination and pathology.[11,12] In addition, DENV NS1 has been shown to increase circulating levels of glycocalyx constituents including sialic acid, hyaluronic acid, heparan sulfate, and syndecan-1 *in vitro* and in animal models.[13,14] However, while YFV NS1 can trigger endothelial dysfunction *in vitro* and in animal models,[8] a direct correlation of NS1 levels with severe YF disease in humans has not been demonstrated.

Syndecan-1, also known as CD138, is an extracellular matrix receptor and a member of the transmembrane heparan sulfate proteoglycan family. Syndecan-1 is involved in many cellular functions, including cell–cell and cell–matrix adhesion, and is highly expressed by epithelial, endothelial, and hematopoietic cells.[15,16] As a part of normal cell surface proteoglycan turnover, the ectodomain of syndecan-1 is constitutively shed from the cell surface via proteolytic cleavage by metalloproteinases.[17] Increased levels of soluble syndecan-1 have been detected in response to injury or infection, and soluble syndecan-1 is often utilized as a marker for glycocalyx disruption. Further, soluble syndecan-1 has been identified as a potential prognostic factor in cancer and systemic inflammatory and autoimmune diseases.[15,16,18] In addition, increased serum levels of syndecan-1 have been associated with higher mortality in COVID-19 patients[19] and severe plasma leakage in dengue patients due to the destruction of the glycocalyx associated with vascular leak.[20–23]

In this study, we use a well-defined cohort of patients with YFV infection to examine the relationship between levels of YFV NS1, soluble syndecan-1, and severe disease manifestations. We found significantly higher levels of YFV NS1 and syndecan-1 in sera of severe YF patients as compared to non-severe YF and control groups. YFV NS1 and syndecan-1 serum levels correlated with each other and with clinical laboratory signs of severe YF disease. We also found that treatment of endothelial monolayers with serum from individuals with severe YF induced significantly higher levels of endothelial permeability as compared to the non-severe YF and control groups. Further, YFV NS1 treatment of endothelial cells induced syndecan-1 shedding, as observed by immunofluorescence and ELISA assays. Together, these results provide further evidence for endothelial dysfunction as a pathogenic mechanism in YFV infections in humans.

Methods

Ethics statement

The yellow fever study was approved by the Institutional Review Board (IRB) of the University of São Paulo (approval # CAAE 59542216.3.1001.0068). The dengue study was approved by the IRB of the Hospital das Clínicas-University of São Paulo (approval # CAPPesq 0652/09). All participants signed written informed consent to be enrolled in the study.

Study participants

This study utilized convenience sampling by gathering all samples available from patients with YF cases confirmed by detection of YFV genomic RNA in plasma and/or autopsy tissues by qRT-PCR, as previously described.[2] Patients were enrolled at the Hospital das Clínicas, School of Medicine, University of São Paulo, Brazil, during an observational cohort study from January 2018 through February 2019[2] (Table 1). Blood samples were collected at the time of admission after informed consent and before any treatment intervention or diagnostic procedures. Blood samples were used for clinical laboratory tests including determination of viral load; leukocyte and platelet counts; levels of hemoglobin, aspartate transaminase (AST), alanine aminotransferase (ALT), creatinine, fibrinogen, and total (TB), direct (DB), and indirect (IB) bilirubin; and coagulation time. Cases were classified in three groups, as follows: i) non-severe (N = 18): individuals who presented viral load $<10^5$ genomic copies/mL, neutrophil count < 4000/mL, AST < 3500 U/L, creatinine < 2.36 mg/mL, and IB < 0.64 mg/dL and who recovered; ii) severe (N = 39): individuals who presented one or more of the following criteria: viral load $\geq 10^5$ genomic copies/mL; neutrophil count ≥4000/mL, AST ≥3500 U/L, creatinine ≥2.36 mg/mL, IB ≥ 0.64 mg/dL, and/or death; iii) controls (N = 11): healthy individuals. Control sera were from healthy blood donors (Table 1). We would like to note that the condition of sample availability depended on the sample volume, and while the samples were not randomly selected, their selection did not depend on exposure factors such as YFV NS1 or syndecan-1 levels, or transendothelial electrical resistance (TEER). A post-hoc power analysis based on 39 severe cases and 18 non-severe cases indicated a power of 77% to detect large effect sizes, using a Cohen's d of 0.8, an alpha level of 0.05, and a two-tailed Wilcoxon test. Similarly, for 3-group analyses, our post-hoc power analysis showed an 80% power to detect an effect size of 0.4, with an alpha level of 0.05, and a two-tailed test. TEER analysis was performed with the first set of samples available in the cohort in 2018. Later, when more samples were collected in 2019 and patient data processed, we were able to include more subjects in the syndecan-1 and YFV NS1 ELISAs.

Samples from DENV-infected patients were collected at the Ana Costa Hospital of Santos, São Paulo state, Brazil, during the 2010 dengue outbreak. Samples collected 3–5 days after symptom onset were confirmed as DENV-positive by detection of DENV RNA using qRT-PCR, as described elsewhere.[24] Plasma leakage was identified by physical examination and confirmed by ultrasound or X-ray[25] (Table 2).

Hybridoma production and ELISA and Western blot analysis

Six female BALB/c mice were immunized intraperitoneally three times (at 10, 7, and 3 weeks before fusion) with 10 μg of recombinant YFV NS1 (strain 17D, Native Antigen) diluted 1:1 in Sigma adjuvant system, and a fourth immunization with YFV NS1 alone was performed 4 days before fusion. Splenocytes collected from 6 euthanized mice were fused with A1 myeloma cells, and hybridomas were selected by growth for two weeks in hypoxanthine-aminopterin-thymidine medium and

	Control (n = 11)	Non-severe (n = 18)	Severe (n = 39)	p-value (Non-severe vs. Severe)
Age (years)	37 (13)	40 (14)	44 (14)	p = 0.50
Sex (female)[a]	7 (64%)	2 (11%)	4 (10%)	p = 0.99
Sex (male)[a]	4 (36%)	16 (89%)	35 (90%)	
Days since symptom onset[b]	–	9 (7–12)	7 (5–9)	p = 0.024
Hospitalization[a]	–	11 (61%)	31 (79%)	p = 0.20
Viral load (genomic RNA copies/mL)	–	1.04×10^3 (7.00×10^3–1.54×10^4)	2.03×10^5 (5.62×10^3–1.68×10^6)	p = 0.00010
Leukocyte count[c]	nd	3.72 (2.69–4.82)	4.22 (3.24–6.37)	p = 0.18
Lymphocyte count[c,d]	nd	1.06 (0.68–1.47)	0.80 (0.52–1.24)	p = 0.11
Neutrophil count[c]	nd	1.74 (1.25–2.93)	2.98 (1.66–5.41)	p = 0.0061
Platelet count[c,d]	nd	89 (60.5–127.5)	67 (44–111)	p = 0.10
Hemoglobin (Hb, g/dL)[d]	nd	13.9 (12.3–15.2)	13.7 (11.6–14.8)	p = 0.55
Hematocrit (Ht, %)[d]	nd	40.9 (35.7–43.7)	39.0 (33.9–42.0)	p = 0.38
Aspartate transaminase (AST, U/L)	nd	522 (389–1265)	3736 (694–7000)	p = 0.00020
Alanine aminotransferase (ALT, U/L)[e]	nd	753 (423–1457)	2232 (843–3366)	p = 0.0060
Creatinine (mg/dL)[f]	nd	0.97 (0.80–1.14)	2.98 (1.04–5.02)	p = 0.00040
Fibrinogen (mg/dL)[g]	nd	184 (139–205)	138 (123–222)	p = 0.22
PT/INR[d]	nd	1.06 (1.00–1.25)	1.30 (1.17–1.91)	p = 0.00010
aPTT (s)[c,f]	nd	30.9 (28.4–33.3)	38.9 (31.2–56.3)	p = 0.0012
Total bilirubin (TB, mg/dL)[d]	nd	1.04 (0.55–3.88)	4.72 (2.31–6.65)	p = 0.0025
Direct bilirubin (DB, mg/dL)[d]	nd	0.92 (0.31–3.46)	4.10 (1.82–5.48)	p = 0.0040
Indirect bilirubin (IB, mg/dL)	nd	0.15 (0.08–0.31)	0.62 (0.31–1.34)	p < 0.0001
Death[a]	–	0 (0%)	17 (43%)	p = 0.0012

Age is shown as mean (SD). Other data are shown as median (IQR). Severe and non-severe groups were compared by one-way ANOVA + Tukey's test (age, parametric) or by Mann–Whitney U test (nonparametric data). Liver transplant was required for one patient from the severe group. nd, not determined; PT/INR: Prothrombin Time/International Normalized Ratio; aPTT, Activated Partial Thromboplastin Clotting Time. [a]Sex (as determined at birth and self-reported by study participants), hospitalization, and death are reported as number of patients per group (percentage of total within each group). [b]All the samples were collected upon hospital admission, and the days since symptom onset was determined based on patient report at admission. [c]Leukocyte, lymphocyte, neutrophil, and platelet count are shown as number × 10^3/mm^3 of blood. [d]Data missing for one patient. [e]Data missing for two patients. [f]Data missing for six patients. [g]Data missing for nine patients.

Table 1: **Demographic, clinical, and laboratory data of study participants from the yellow fever cohort.**

screened with a YFV NS1 antigen-coat ELISA. In brief, Nunc MaxiSorp ELISA plates (Thermo Scientific) were coated overnight with 0.5 μg/mL of YFV NS1 in PBS and blocked the next day for 1 h using PBS containing 5% nonfat dry milk, washed twice with PBS, and incubated with hybridoma supernatant for 1 h at room temperature. Plates were washed 3X with PBS-Tween 20 0.01% (PBS-T) and 2X with PBS, and horseradish peroxidase (HRP)-conjugated secondary antibody diluted in PBS-BSA 1% was added for 1 h. After washing with PBS-T, 3,3′,5,5′-Tetramethylbenzidine (TMB) liquid substrate (Sigma) was added and left to develop for 10 min. Two-fold titrations from 1:100 to 1:6400 of polyclonal sera collected from NS1-immunized mice were used as a positive control in the NS1 antigen-coated ELISA. Plates were read at optical density (OD) of 450 nm using a BioTek/Agilent microplate reader. The monoclonal antibodies (mAbs)

	Control (n = 11)	Dengue no leak (n = 7)	Dengue leak[a] (n = 7)	p-value (no leak vs. leak)
Age (years)	37 (13)	35 (21)	25 (16)	p = 0.21
Sex (female)[b]	7 (64%)	3 (43%)	5 (71%)	p = 0.59
Sex (male)[b]	4 (36%)	4 (57%)	2 (29%)	
Days since symptom onset[c]	–	4 (3–4)	3 (3–4)	p = 0.59
Hospitalization[b]	–	0	7 (100%)	p = 0.00060
Platelet count[d]	nd	152 (81–179)	40 (28–46)	p = 0.0012

Age is shown as mean (SD). Days of symptoms and platelets counts are shown as median (IQR). Dengue no leak and leak groups were compared by one-way ANOVA + Tukey's test (age, parametric) or by Mann–Whitney U test (nonparametric data). No patients died in this cohort. nd, not determined. [a]Dengue leak group corresponds to patients diagnosed with plasma leakage by physical examination and confirmed by ultrasound or X-ray.[25] [b]Sex (as determined at birth and self-reported by study participants) and hospitalization are reported as number of patients per group (percentage of total within each group). [c]All the samples were collected upon hospital admission, and days since symptom onset were determined based on patient report at admission. [d]Platelet count is shown as number × 10^3/mm^3 of blood.

Table 2: **Demographic, clinical, and laboratory data of study participants from the dengue cohort.**

with the highest OD value and shortest growth doubling time were selected for expansion and purification. Cells from ELISA-positive wells were cloned and expanded before being tested by ELISA for YFV specificity using 12 recombinant flavivirus NS1 proteins obtained from Native Antigen Company: YFV; dengue virus serotypes 1 (DENV1), 2 (DENV2), 3 (DENV3), and 4 (DENV4); Saint Louis encephalitis virus (SLEV); West Nile virus (WNV); Zika virus (ZIKV); Wesselsbron virus (WBV); Usutu virus (USUV); Japanese encephalitis virus (JEV); and tick-borne encephalitis virus (TBEV).[26] Our previously described pan-flavivirus anti-NS1 mouse immunoglobulin G2b (IgG2b) mAb, 2B7, was used as a control for ELISA and WB experiments.[27]

The YFJ19 mAb was tested by Western blot for specificity to YFV NS1. The same 12 recombinant flavivirus NS1 proteins used above were separated on a 10% polyacrylamide gel and transferred onto nitrocellulose membranes. Membranes were incubated overnight with 7 mL of hybridoma supernatant or 3.5 μL of mouse anti-His mAb (Abcam) as a control in PBS-T containing 5% nonfat dry milk. After antibody incubation, membranes were washed 4X with PBS-T and then probed with anti-mouse secondary antibodies conjugated to HRP (Biolegend) for 1 h. Membranes were then washed 4X with PBS-T, developed using ECL reagents, imaged on a ChemiDoc system, and analyzed using Image Lab software (Bio-Rad).

Monoclonal antibody (mAb) purification

Hybridoma supernatant in batches of 400 mL was filtered using a 0.22 μm pore size bottle-top vacuum filter (Corning) to remove cell debris. Buffers were prepared based on the manufacturer's recommendations (Cytiva Protein G Sepharose 4 Affinity Chromatography Handbook). Next, supernatant was diluted 1:1 with binding buffer (20 mM $H_2NaO_4P{\cdot}H_2O$, pH 7.0). Protein G resin (2.5 mL, Cytiva Protein G SepharoseTM 4 Fast Flow) was added to a 1.0 × 10 cm Econo-Column (Bio-Rad) and washed twice with 10 mL of binding buffer. Supernatant/binding buffer solution was added to a Econo-Column Reservoir (Bio-Rad) attached to the Econo-Column and allowed to gravity flow through the resin. After flow-through was collected, the resin was washed twice with 10 mL of binding buffer to remove supernatant. To elute the bound mAbs, 6 mL of elution buffer (0.1 M glycine buffer, pH 2.5–3.0) was added to the column. Elution fractions were collected in 1-mL fractions and diluted 1:10 with neutralizing buffer (1 M TrisHCl, pH 9.0). mAb concentration was calculated using a Nanodrop spectrophotometer, and the top yields were selected and pooled. Purified mAbs were dialyzed using a Slide-A-Lyzer 10 K (Fisher) over 48 h at 4 °C with two separate exchanges of PBS buffer.

YFV NS1 capture ELISA

ELISA plates were coated with 5 μg/mL of capture mAb YFJ19 in 50 μL PBS/well and incubated at 4 °C overnight. The next day, plates were washed once with PBS and blocked with PBS-BSA 3% (100 μL) and incubated for 1 h at room temperature. The plate was then washed twice with PBS-T, and the serum samples (1:5 dilution) or recombinant NS1 were both diluted in PBS-BSA 1% before being added to the plate and incubated for 2 h at room temperature. Plates were washed 4X with PBS-T, and the biotinylated detecting mAb YFJ19 (Pierce Antibody Biotinylation Kit for IP, ThermoFisher) was diluted 1:1000 in PBS-BSA 1% (50 μL) and added to the plate to incubate for 1 h at room temperature. The plate was then washed 4X with PBS-T. HRP-streptavidin (Jackson Immuno) diluted 1:200 in PBS-BSA (50 μL) was then added to the plate and incubated at room temperature for 1 h. After incubation, the plate was washed 4X with PBS-T and 1X with PBS. The plate was then developed with TMB substrate (100 μL; Sigma). The enzymatic reaction was stopped after 15 min using 2 N H_2SO_4, and the plate was read at OD 450 nm. The concentrations of NS1 in sera were interpolated using a standard curve of recombinant NS1 ranging from 1 to 1000 ng/mL; the limit of detection for this assay was 2 ng/mL.

Determination of syndecan-1 levels in human serum

The amount of syndecan-1 in serum was determined using the human syndecan-1 DuoSet ELISA Kit (DY2780, R&D Systems). Briefly, 96-well ELISA microplates were coated with 80 ng/well of goat anti-human syndecan-1 capture antibody overnight at room temperature. After washing and blocking with 1% bovine serum albumin (BSA), plates were incubated with samples (YF patients, dengue patients, or healthy controls) diluted 1:25 or recombinant human syndecan-1 standards for 2 h. After washing, plates were incubated with 5 ng/well of biotinylated goat anti-human syndecan-1 detection antibody. After 2 h, HRP-streptavidin was added for signal detection with TMB substrate. The OD 450 nm with a correction at OD 550 nm was determined using a Bio-Tek/Agilent microplate reader. Syndecan-1 levels were determined by interpolation analysis of standard curves with four-parameter logistic regression.

Evaluation of endothelial barrier function *in vitro*

To evaluate the putative effects of acute-phase serum from YFV-infected patients on endothelial barrier function, we used the TEER assay as described previously.[25,27] In brief, human umbilical vein endothelial cells, kindly donated by Dr. Miriam Fonseca-Alaniz (Instituto do Coração, InCor, University of São Paulo, Brazil) were seeded (6×10^4 cells/well) in Transwell polycarbonate membrane inserts (0.4 μm pore, 6.5 mm diameter; Corning Inc.) in endothelial cell growth basal medium 2 supplemented with an Endothelial Cell Growth Medium-2 (EGM-2TM) supplemental bullet kit (Lonza). After 72 h of incubation at 37 °C and 5% CO_2,

cells were treated with human sera (10% final vol/vol concentration) obtained from YFV-positive severe and non-severe patients or YFV-negative blood donors (healthy controls). TEER values, expressed in Ohms (Ω), were collected at sequential 2-h time-points 2–10 h following treatments using an Epithelial Volt Ohm Meter (EVOM) with a "chopstick" electrode (World Precision Instruments). Resistance of inserts with no cells (blank) and inserts with cells (untreated) containing medium alone, were used to calculate relative TEER as a ratio of the corrected resistance values as (Ω experimental condition - Ω blank)/(Ω untreated - Ω blank). Recombinant YFV NS1 (Native Antigen Co.) at 10 μg/mL was used as a positive control.

Measurement of syndecan-1 and sialic acid levels on the surface of human endothelial cells by immunofluorescence assay (IFA) and soluble syndecan-1 levels in cell supernatants by ELISA

Human pulmonary microvascular endothelial cells (HPMEC ST1-6 R, a gift from J.C. Kirkpatrick, Johannes-Gutenberg University) or human hepatic sinusoidal endothelial cells (HHSEC, Sciencell, catalog # 5000) were seeded (1×10^5 cells) on gelatin-coated coverslips and allowed to grow until full confluency was attained (approximately 3 days). On the day of the experiment, cells were treated or not with 10 μg/mL of YFV NS1 protein and incubated for 6 h at 37 °C. After incubation, supernatants were collected, and cells were washed and fixed with 4% paraformaldehyde for 10 min. For detection of surface levels of syndecan-1, HPMECs were stained overnight with 2 μg/mL of rabbit anti-syndecan-1 IgG antibody (Abcam, ab188861). After washing, secondary staining was performed by adding 2 μg/mL of donkey anti-rabbit IgG conjugated to Alexa Fluor 647 (Abcam, ab150075) for 4 h. Nuclei were stained using Hoechst (ImmunoChemistry Technologies). To detect syndecan-1 in HPMEC supernatants, the same Human Syndecan-1 DuoSet ELISA kit (R&D Systems, catalog # DY2780) was used as described earlier. To detect sialic acid on the surface of HHSEC, fixed cells were treated with 5 μg of the sialic acid-specific lectin, wheat germ agglutinin (WGA), conjugated to Alexa Fluor 647 (Thermo Fisher Scientific).[14] Mounted slides were imaged on a Zeiss LSM 710 Axio Observer fluorescence microscope (CRL Molecular Imaging Center, UC Berkeley). Images acquired using the Zen 2010 software (Zeiss, Jena, Germany) were processed and analyzed with ImageJ software.[28] Mean fluorescence intensity (MFI) values for syndecan-1 and sialic acid staining were obtained from individual RGB-grayscale-transformed images (n = 3).

Statistics

ELISA values were modeled using 4-parametric logistic regression, using dilution as predictor and OD as the response values to fit sigmoidal (S-shaped) curves to data. Parameters of the models were maximum value, minimum value, inflection point (50% of the effect), and the Hill slope.[29] Spearman's rank correlation was used to determine the relationship between two continuous variables non-parametrically.[30] Linear models were used exclusively to visualize the relationship between continuous values of relevant biomarkers [YFV NS1, soluble syndecan-1, and TEER (AUC)], and no covariates were considered.[31] Locally estimated scatterplot smoothing (LOESS) models were used to visualize the trend of relevant biomarkers over days since symptom onset.[26] LOESS models were implemented using a span = 1. The span was determined based on the best visualization that accounts for the low sample size and large gaps between the sample days. R-squared (R^2) was computed from the sum of the squares of the distances of the points from the best–fit curve determined by nonlinear regression.[32] The calculation of the residual sum of squares (SSreg) involved determining the best–fit curve through nonlinear regression and then summing the squares of the vertical distances between each data point and the best–fit curve. SSreg was expressed in the squared units of the Y-axis variable. To convert the R^2 into a fraction that ranges between 0 and 1, SSreg was normalized by the total sum of squares (SStot). SStot represents the total variance in the data and is calculated by summing the squares of the distances from each data point to a horizontal line that corresponds to the mean value of the dependent variable (Y-axis). R^2 was calculated by subtracting the division of the SSreg by the SStot from 1 ($R^2 = (1 - \text{Ssreg})/\text{SStot}$).

Data were analyzed using R language version 4.1.1 within the RStudio (2021.09.0, Build 351) integrated development environment. Plots were visualized using the base R graphics and ggplot2 (v3.3.5) package. Groups were compared using parametric (t-test or ANOVA) or non-parametric tests (Mann–Whitney U or Kruskal–Wallis tests), according to the data normality and homogeneity of variances, with a significance level of 0.05. The median differences between groups and 95% confidence intervals (CIs) were estimated by Hodges-Lehmann and Mann–Whitney U tests, respectively. Statistical tests used in each comparison are indicated in the corresponding figure legends. Resultant *p*-values from the above statistical tests are displayed in the figures. All statistics not indicated are not significant.

Role of the funding source

Authors declare that sponsors of this study had no role in the study design, collection, analysis, and interpretation of data, nor in the writing of the report and the decision to submit the paper for publication.

Results

Characteristics of study participants

In this study, we analyzed serum samples from individuals with suspected YF collected at the time of

hospital admission during an observational cohort study initiated during the 2018 YF epidemic in São Paulo, Brazil, as previously described,[2] and continued through the subsequent epidemic in 2019. Demographic characteristics, clinical manifestations, and laboratory data of study participants with RT-PCR-confirmed YF cases as well as healthy controls are provided in Table 1. We used the laboratory criteria (viral load, neutrophil count, AST, creatinine, and indirect bilirubin [IB]) previously determined to predict mortality in YF patients from the same cohort,[2] or death, to define severe cases. Table 1 shows that in addition to these criteria, severe YF cases also displayed significantly higher levels of ALT, total bilirubin (TB), and direct bilirubin (DB), as well as increased prothrombin time (PT/INR) and activated partial thromboplastin time (aPTT), when compared to the non-severe group. The majority of YF-positive study participants were male agriculture or forestry workers. We also tested a small set of serum samples from dengue patients in the syndecan-1 ELISA assay. These were separated in two groups, according to occurrence or not of diagnosed plasma leakage (Table 2).

Development of a quantitative YFV NS1 capture ELISA for clinical samples

YFV NS1 has been previously implicated as a direct trigger of endothelial dysfunction and vascular leak *in vitro* and in mouse models.[8] Although DENV NS1 has been shown to be associated with disease severity,[5–7] little is known about the contribution of YFV NS1 to pathogenesis in humans. To measure YFV NS1 levels in the serum of infected patients, we established a quantitative YFV NS1 capture ELISA using an in-house-produced mouse anti-YFV-NS1 mAb. After testing different mAbs, YFJ19 (IgG1) used as the capture mAb and biotinylated YFJ19 as the detection mAb was determined to be the optimal combination, displaying the highest signal and specificity for YFV NS1 (Supplementary Fig. S1). Standard curves were generated via ELISA with recombinant YFV NS1 concentrations (0.24–2000 ng/mL) vs. absorbance values (Fig. 1a), with no significant changes observed when human serum (1:10) was added (Fig. 1b), indicating that the assay could be performed with clinical samples. Although linearity assumption was not assessed, R^2 was used to determine how well the model fit the data. Unweighted R^2 values were calculated according to the method of Kvalseth.[32] We found R^2 values > 0.99 for the 4-parameter logistic regressions performed (Fig. 1a and b), indicating a high goodness of fit. The analytic detection range was 2–500 ng/mL. YFJ19, as well as 2B7, a pan-flavivirus anti-NS1 mAb, was tested across a panel of 12 flavivirus NS1 proteins using both direct ELISA and Western blot methods. Results show that YFJ19, in contrast to 2B7, was specific to YFV NS1 (Fig. 1c, d, e; Supplementary Fig. S2). This specificity is important for assays detecting flavivirus NS1, especially because different flaviviruses can co-circulate in endemic areas such as Brazil.

NS1 serum levels are significantly increased in severe YF

Using our in-house ELISA, we found that YFV NS1 levels were significantly higher in the severe YF group (median = 77.6 ng/mL, 95% CI 73.2–164.5) compared to the non-severe group (median = 0 ng/mL, 95% CI −6.9 to 65.8, difference estimate: −58.9, $p = 0.0028$) and to the control group (no NS1 detected, median = 0 ng/mL, 95% CI 0 - 0, difference estimate: −77.5, $p = 0.018$) (Fig. 2a). We also observed trending higher levels of YFV NS1 when comparing the deceased (median 67.0 ng/mL, 95% CI 47.5–230) to the surviving group (median 0 ng/mL, 95% CI 39.0–106.8, difference estimate: −77.5, $p = 0.061$; Fig. 2b). YFV NS1 serum levels were observed to be highest between 5 and 13 days post-symptom onset (Fig. 2c).

Serum levels of syndecan-1 correlate with disease severity in YF patients

Because soluble syndecan-1 is a biomarker for endothelial injury in multiple diseases, we quantified syndecan-1 in the serum samples of our cohort. We found significantly increased soluble syndecan-1 levels in severe (median 177.1 ng/mL, 95% CI 130.2–186.3, difference estimate: −96.5, $p = 0.0045$) vs. non-severe (median 41.2 ng/mL, 95% CI 35.1–110.9) YF cases and significantly higher levels in both severe (difference estimate: −173.5, $p < 0.0001$) and non-severe (difference estimate: −30.56, $p = 0.011$) YF groups when compared to healthy controls (Fig. 3a). Importantly, serum syndecan-1 levels were also significantly higher in individuals who succumbed (median 235 ng/mL, 95% CI 195.2–238.9) compared to those who survived (median 57.44 ng/mL, 95% CI 69.3–122.5, difference estimate: −135.8, $p < 0.0001$) (Fig. 3b). These findings indicate that endothelial dysfunction is associated with disease severity in YFV-infected patients and that soluble syndecan-1 can be used as a biomarker of YF disease severity. Similar to YFV NS1, syndecan-1 serum levels were highest 4–13 days after symptom onset (Fig. 3c). As expected, we also found that syndecan-1 levels, when compared to the same healthy controls as above, were significantly increased in serum samples from dengue patients with diagnosed vascular leak (median 38.0 ng/mL, 95% CI 7.9–87.9, difference estimate: −34.3, $p < 0.0001$) (Fig. 3d).

Sera from patients acutely infected with YFV induce endothelial dysfunction *in vitro*, correlating with disease severity

To evaluate the capacity of serum from YF patients to mediate endothelial hyperpermeability, we evaluated the transendothelial electrical resistance (TEER) of human

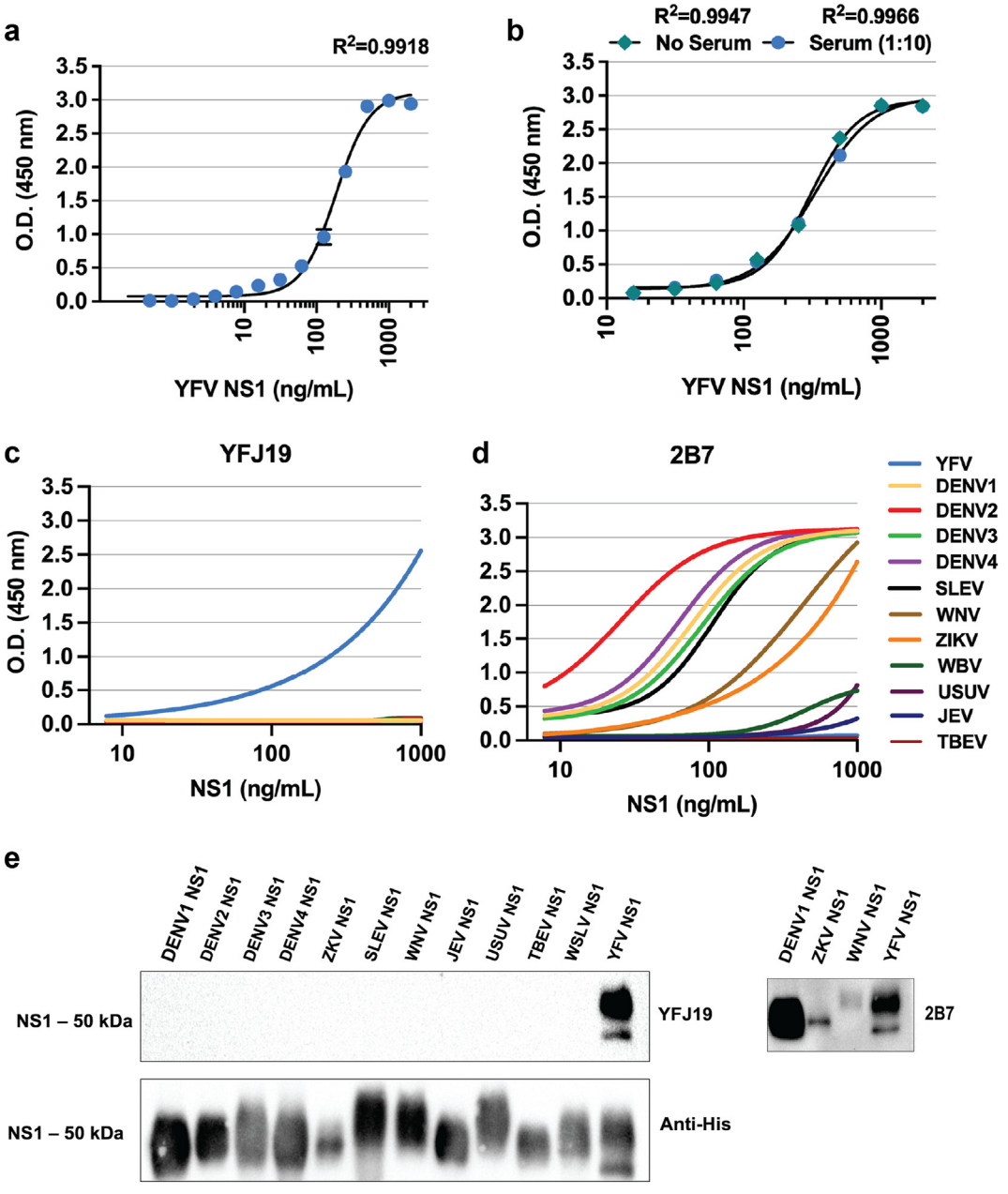

Fig. 1: Development of quantitative YFV NS1 ELISA. (a) Sigmoidal standard curve of YFV NS1 capture ELISA performed with in-house-produced YFJ19 mAb and thirteen different concentrations of recombinant YFV NS1. The graph depicts mean absorbance values ± standard deviation (SD). (b) Comparison of standard curve of YFV NS1 diluted or not in normal human serum (1:10). The graph depicts mean absorbance values ± SD. (c) Specificity of mAb YFJ19 by direct ELISA performed with NS1 (5 µg/mL) from 12 different flaviviruses as follows: YFV; dengue virus serotypes 1 (DENV1), 2 (DENV2), 3 (DENV2), and 4 (DENV4); Saint Louis encephalitis virus (SLEV); West Nile virus (WNV); Zika virus (ZIKV); Wesselsbron virus (WBV); Usutu virus (USUV); Japanese encephalitis virus (JEV); Tick-borne encephalitis virus (TBEV). (d) Cross-reactivity of anti-flavivirus NS1 mAb (2B7) by direct ELISA performed with NS1 (5 µg/mL) from the 12 different flaviviruses as in c. (e) Western blot analysis showing specificity of mAb YFJ19 for YFV NS1 and cross-reactivity of mAb 2B7.

endothelial cells cultured in Transwell inserts and treated with sera from the different groups. We found that mean relative TEER values of severe and non-severe YF groups were reduced in comparison to medium-only or control groups, indicating that serum components were capable of inducing varying degrees of endothelial

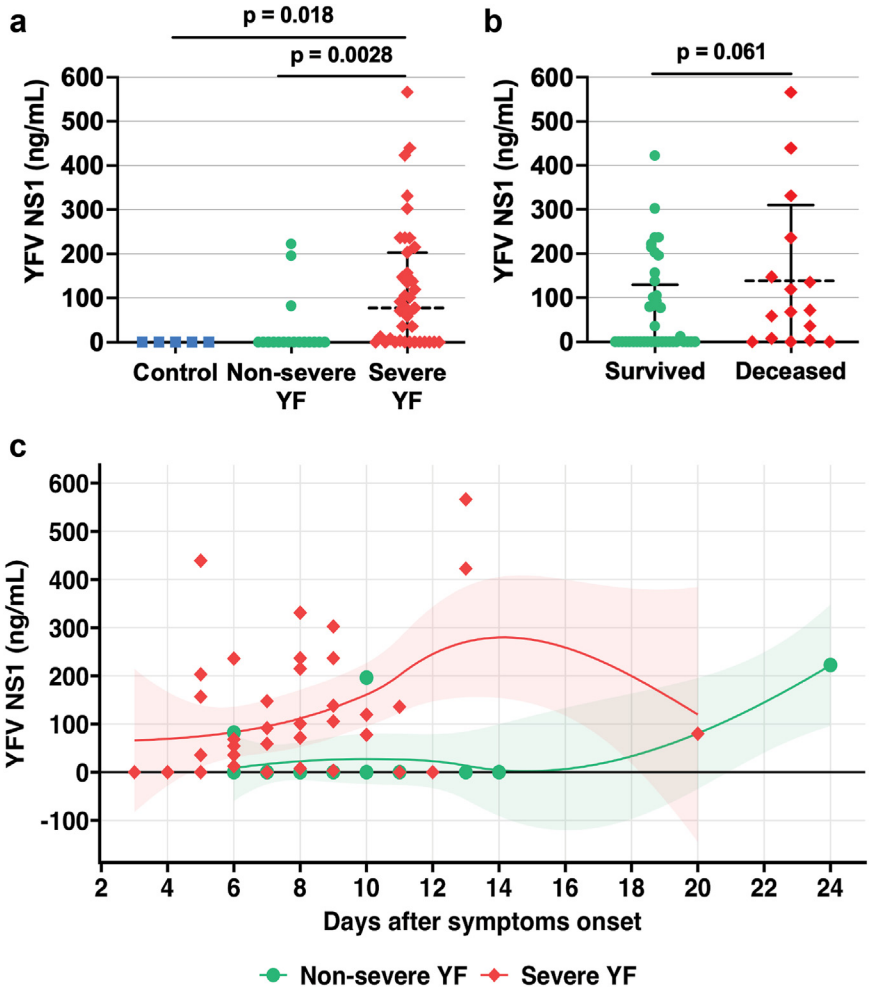

Fig. 2: YFV NS1 serum levels in severe and non-severe YF patients. (a) YFV NS1 levels were determined using an in-house sandwich ELISA, as described in Materials and Methods. Studied individuals were classified in three different groups as described in Materials and Methods: Severe YF (n = 39); Non-severe YF (n = 17, missing data for 1 sample); Controls, healthy individuals (n = 5, missing data for 6 samples). Groups were compared by Kruskal–Wallis + Dunn's multiple comparisons test. (b) YFV NS1 levels in survivors and deceased YFV-infected groups. Groups were compared by Mann–Whitney test. The dashed lines indicate the median of the data, and the error bars represent the interquartile range (IQR) in a and b. (c) YFV NS1 serum levels in individuals with acute YF according to days since symptom onset, visualized using LOESS curves with 95% confidence intervals (shaded areas). Acute disease was defined by detection of viral RNA by RT-qPCR in serum. Samples were run in duplicate.

hyperpermeability according to disease severity (Fig. 4a). Comparing the area under the curve (AUC) of TEER nadirs, the severe (median 0.96, 95% CI 0.82–2.2) YF group displayed significantly greater values when compared to both non-severe (median 0.26, 95% CI 0.12–1.03, difference estimate: –0.50, $p = 0.040$) YF and control (median 0, 95% CI –0.01 to 0.04, difference estimate: –0.94, $p < 0.0001$) groups (Fig. 4b). Similarly, recombinant YFV NS1, used as a positive control, induced endothelial dysfunction, resulting in reduction of relative TEER values (Fig. 4a and b). The TEER curves for each sample are shown in Supplementary Fig. S3.

YFV NS1 induces syndecan-1 and sialic acid shedding in human endothelial cells

To evaluate the capacity of YFV NS1 to serve as a direct trigger of endothelial dysfunction, we measured the effect of NS1 on syndecan-1 levels on a monolayer of human endothelial cells. Consistent with our observed correlation between YFV NS1 and soluble syndecan-1 in clinical samples, we found that recombinant YFV NS1 treatment of endothelial cells resulted in a significant reduction of cell surface-bound syndecan-1 relative to the medium-only control as detected by immunofluorescence assay (IFA) (Fig. 4c and d) and

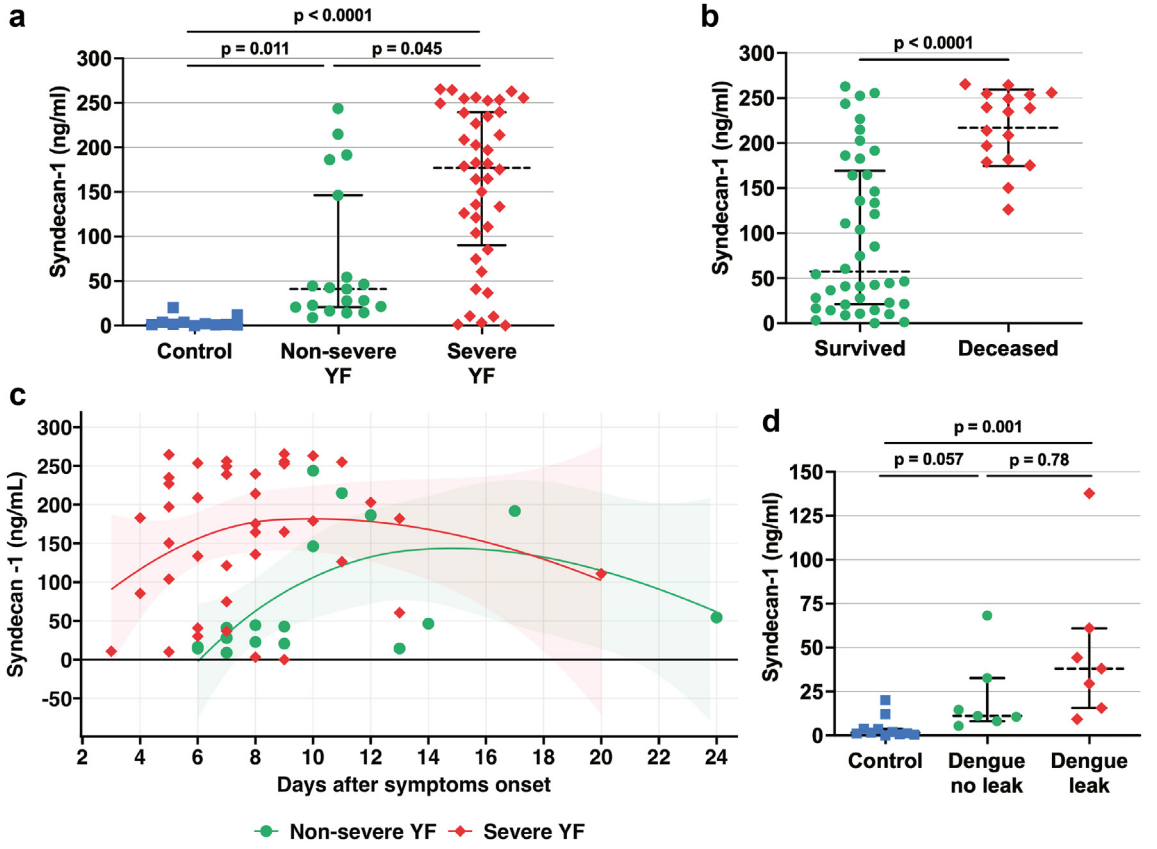

Fig. 3: Syndecan-1 levels in sera of individuals with acute YF and dengue. (a) Syndecan-1 levels in sera were determined by the human syndecan-1 ELISA Kit. Studied individuals were classified in three different groups as described in Materials and Methods: Severe YF (n = 39); Non-severe YF (n = 18); Controls (n = 11): healthy individuals. Groups were compared by Kruskal–Wallis + Dunn's multiple comparisons test. (b) Syndecan-1 serum levels in survivors and deceased individuals from the YFV-infected groups, compared by Mann Whitney test. (c) Syndecan-1 serum levels in individuals with acute YF according to days since symptom onset, visualized using LOESS curves with 95% confidence intervals (shaded areas). (d) Syndecan-1 serum levels in individuals with acute DENV infection. Dengue no leak (n = 7): individuals with acute dengue who did not display plasma leakage; Dengue leak (n = 7): individuals with acute dengue who displayed plasma leakage; Controls (n = 11): same healthy individuals as shown in panel A. Soluble syndecan-1 levels in dengue groups were compared by Kruskal–Wallis + Dunn's multiple comparisons test. The dashed lines indicate the median of the data, and the error bars represent the interquartile range (IQR) in a, b, and d. Acute disease was defined by detection of viral RNA by RT-qPCR in serum. Samples were run in duplicate.

increased levels of syndecan-1 in the cell supernatant as measured by ELISA (Fig. 4e). We also tested endothelial cells treated with YFV NS1 in the presence or absence of polyclonal sera from mice vaccinated with YFV NS1 (strain 17D). We utilized polyclonal sera because YFJ19 does not bind to a functional epitope of YFV NS1 (data not shown). We found that our anti-YFV NS1 polyserum inhibited the capacity of YFV NS1 to trigger shedding of syndecan-1 from the surface of HHSEC, providing evidence for specificity of our barrier dysfunction phenotype (Fig. 4e). Another glycocalyx component, sialic acid, was also observed to be reduced on the cell surface after YFV NS1 treatment (Fig. 4f and g). These data support that circulating YFV NS1 could be a contributing factor to endothelial dysfunction in YF patients.

TEER, syndecan-1, and YFV NS1 serum levels correlate with clinical and laboratory parameters of severe YF

We next performed a correlation matrix analysis of patient data and results regarding TEER, syndecan-1 and YFV NS1 serum levels (Fig. 5a, with significant [$p < 0.05$, $r > 0.35$] correlations indicated with asterisks). Importantly, we found that YFV NS1 levels correlated with serum syndecan-1 levels, TEER values, neutrophil count, hematocrit (Ht), and IB (Fig. 5a, b, c). Further, serum syndecan-1 levels correlated significantly with YFV NS1, TEER values, sex (male), hospitalization, viral load, parameters of liver impairment (AST, ALT, creatinine, TB, DB, and IB), kidney dysfunction (creatinine), coagulopathy (fibrinogen, PT/INR, aPTT), and death (Fig. 5a–d). TEER values correlated with YFV NS1,

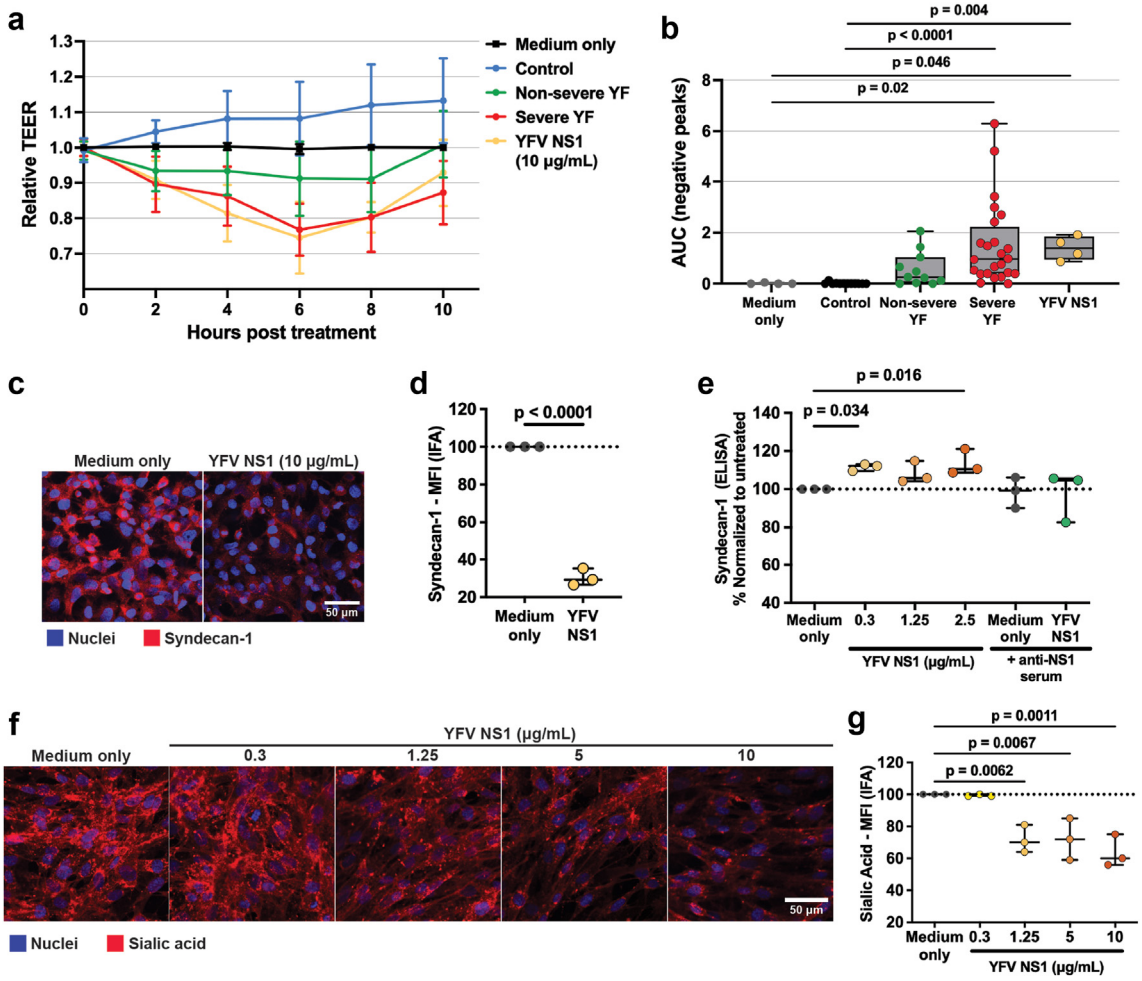

Fig. 4: Relative TEER of human endothelial cells treated with acute YF human serum samples and effects of YFV NS1 treatment on endothelial glycocalyx. (a) Confluent monolayers of human endothelial cells cultured in Transwell inserts were treated or not with 10% serum from three different groups: Severe YF (n = 24, missing data for 15 samples); Non-severe YF (n = 10, missing data for 8 samples); Controls (n = 11): healthy individuals. YFV NS1 (10 µg/mL) was used as positive control. The transendothelial electrical resistance (TEER) was measured from 2 to 10 h post-treatment. Graph shows mean ± SD of relative TEER for each treatment group. (b) Area under the curve (AUC) of negative peaks for the effects of the different treatments on TEER. AUC values represent the sum of the trapezoidal areas (taking into account only the negative peaks) under the curve formed by the data points. Median values of AUC for each group were compared using Kruskal–Wallis' test. Error bars represent interquartile range (IQR). Outliers were defined according to Tukey's method, which identifies outliers using the interquartile range (IQR; i.e., the difference between the first and third quartiles [Q3 - Q1]) as any data point below the first quartile (25th percentile) minus 1.5 times the IQR (Q1 - 1.5*IQR) or above the third quartile (75th percentile) plus 1.5 times the IQR (Q3 + 1.5*IQR). (c, d) Human endothelial cell monolayers grown on gelatin-coated coverslips were treated with medium only or 10 µg/mL of YFV NS1 for 3 h. After fixation, cell surface syndecan-1 was stained in red and nuclei in blue (Hoechst). (c) Representative figures of cell monolayers stained for syndecan-1 in red and nuclei in blue. (d) Quantification of syndecan-1 protein on the cells surface expressed as mean fluorescence intensity (MFI). NS1 treatment was compared to medium-only treatment by unpaired t-test. Error bars present SD of the mean. (e, f, g) Human endothelial cell monolayers grown on gelatin-coated coverslips were treated with medium only or with different concentrations of YFV NS1 for 6 h. (e) Quantification of syndecan-1 in cell supernatants by ELISA. An in-house-produced mouse anti-YFV NS1 polyserum with or without 2.5 µg/mL of YFV NS1 was used as a control. Treatments were compared with medium-only treatment by one-way ANOVA + Dunnett's test. Error bars present SD of the mean. (f) Representative figures of cell monolayers stained for sialic acid in red and nuclei in blue. (g) Quantification of sialic acid on the cell surface expressed as MFI. NS1 treatments were compared to medium-only treatment by one-way ANOVA + Dunnett's multiple comparison test. Error bars present SD of the mean. Significant *p*-values are shown in the graphs. Acute YF disease was defined by detection of viral RNA by RT-qPCR in serum. Samples were run in duplicate for the TEER assays. IFA and ELISA data are the results of three independent experiments (n = 3).

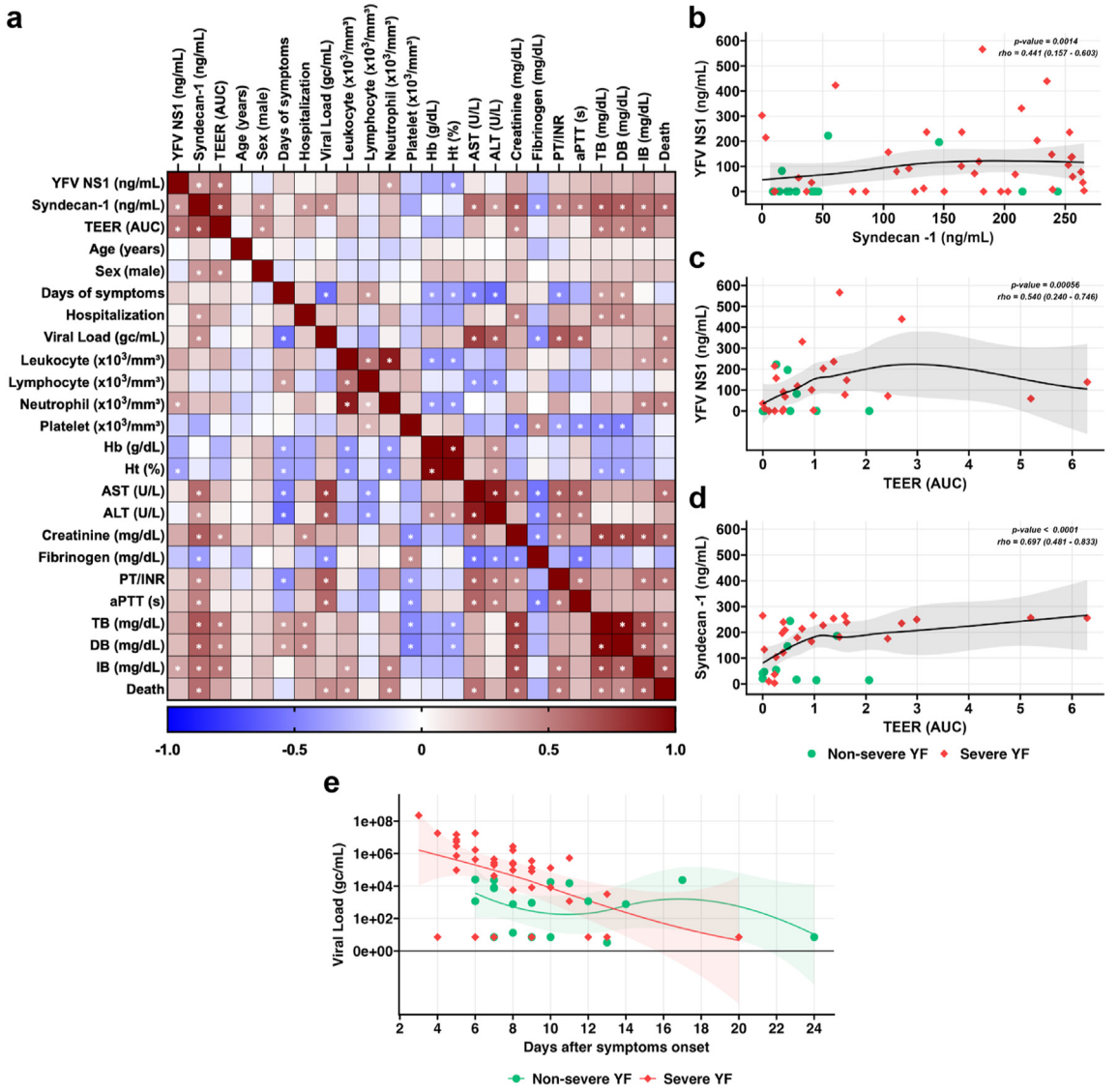

Fig. 5: Correlation analysis of clinical and laboratory data of study participants during acute YF and viral load according to days of symptoms. (a) Correlation matrix analyzed by Spearman rank correlation. Asterisks indicate significant correlations ($p < 0.05$, Spearman $r > 0.35$). Categorical variables (e.g., sex [male] and death) were entered as coded variables. (b) Correlation between serum levels of YFV NS1 and syndecan-1. (c) Correlation between serum levels of YFV NS1 and TEER AUC values. (d) Correlation between serum levels of syndecan-1 and TEER AUC values. The gray shaded area represents the 95% confidence interval for the fitted LOESS curve in b, c, and d. Abbreviations: TEER, transendothelial electrical resistance; AUC, area under the curve; Hb, hemoglobin; Ht, hematocrit; AST, aspartate transaminase; ALT, alanine aminotransferase; TPI/INR thrombin potential index/international normalized ratio; aPTT, activated partial thromboplastin time; TB, total bilirubin; DB, direct bilirubin; IB, indirect bilirubin. (e) Viral load of YF patients from severe and non-severe cases. Viral load, determined in YF patients serum at the time of admission by RT-qPCR, is expressed as genomic copies per mL. Results were plotted according to days since symptom onset reported at the time of hospital admission. Acute disease was defined by detection of viral RNA by RT-qPCR in serum.

syndecan-1, sex (male), creatinine, TB, DB, and IB (Fig. 5a–c, d). Results of viral load according to days of symptoms onset are depicted in Fig. 5e. These findings show that TEER values and serum levels of YFV NS1 and syndecan-1 correlated with each other and with clinical laboratory parameters of disease severity, suggesting a potential link between YFV NS1 and endothelial dysfunction, resulting in increased shedding of syndecan-1.

Discussion

We previously demonstrated *in vitro* and in mouse models that YFV NS1 mediates endothelial dysfunction

and hyperpermeability, triggering breakdown of the glycocalyx via enzymatic activation.[8] In this study, we aimed to further understand the role of endothelial dysfunction in the pathogenesis of human YF. We found that serum levels of both NS1 and syndecan-1 were correlated with multiple clinical laboratory parameters associated with YF disease, providing evidence that YFV NS1 and soluble syndecan-1 may be linked to severe YF disease manifestations. When placing human endothelial cells in contact with sera from different groups of patients, we observed a significant increase in permeability with the severe as compared to non-severe and healthy control groups. We also observed *in vitro* that YFV NS1 induces shedding of syndecan-1 from human endothelial cells and reduction of syndecan-1 and sialic acid in the glycocalyx on the cell surface. Our results highlight the secretion of YFV NS1 from infected cells and endothelial glycocalyx degradation as prominent characteristics of YF pathogenesis in humans and suggest that levels of NS1 and/or levels of soluble syndecan-1 may help assess risk of developing severe illness.

Flavivirus NS1 is an important virulence factor in facilitating flavivirus pathogenesis by triggering enzymatic disruption of the glycocalyx as well as mediating the breakdown of intercellular junctional complexes of endothelial cells, both pathways contributing to tissue-specific vascular leak.[8,9,27] We have previously shown that YFV NS1 treatment induces significant hyperpermeability in human endothelial cells and in mice.[8] Our data here show that severe YF cases displayed higher levels of YFV NS1 as early as 5 days post-disease onset, supporting the concept that production of NS1 by YFV-infected cells may contribute to YF disease. Therefore, measuring the serum levels NS1 using a sensitive and specific assay, such as the capture ELISA developed here, could potentially provide a clinical diagnostic/prognostic marker for YF.

Syndecan-1 is a heparan sulfate proteoglycan expressed on endothelial cells and an established marker of inflammatory disease and glycocalyx damage.[33] Shedding of endothelial glycocalyx components, such as syndecan-1, is a known result of endothelial dysfunction, and increased serum levels of syndecan-1 have been confirmed in patients with diseases such as COVID-19,[19] septic shock,[34] and cancer[35,36] and associated with plasma leakage and disease severity in dengue.[20,21,37,38] Here, we show that higher serum levels of syndecan-1 correlate with severe YF; thus, soluble syndecan-1 may also serve as a biomarker for severe YF disease.

YF is a systemic disease, but the pathology is primarily targeted to the liver. Several studies have described endothelial alteration, showing immunohistochemical analyses of endothelial tissues in the hepatic parenchyma of YF-positive subjects, with increased expression of adhesion molecules such as ICAM-1 and VCAM-1 that result in recruitment and migration of immune cells, contributing to inflammatory processes in the liver of fatal cases and morphological changes such as edema and congestion of the portal tract.[39–41] Previous analysis of autopsy samples performed in four patients who died of YF in the same cohort as that studied here found hepatic edema in the portal tracts and in the space of Disse, observed by electron microscopy analysis.[42] Recently, Giugni et al.[43] performed a retrospective autopsy study to evaluate YF-associated cardiac pathology on samples from fatal cases in the same cohort, including 15 fatal cases also analyzed in our study. The authors found endothelial cell injury, interstitial edema, YFV antigen in the cytoplasm of endothelial cells, and significantly increased levels of biomarkers of vascular inflammatory response in the heart (e.g., syndecan-1, angiopoietin-2, endothelin-1, vascular cell adhesion protein 1, and plasminogen activator inhibitor 1) in comparison to the control group (patients who died from cardiovascular disease). Our present data are in line with this previous evidence of endothelial impairment and elevated levels of syndecan-1 in fatal cases.[39–44]

Although it is difficult to determine the direct activity of soluble NS1 on the endothelium of infected humans, our current results highlight that increased NS1 levels are associated with YF disease severity. Based on our and others' previous work on the mechanism of flavivirus NS1, we hypothesize that secreted YFV NS1 in the bloodstream enables its interaction with endothelial cells, inducing glycocalyx degradation via activation of cathepsin L, heparanase, and matrix metalloproteinases (MMPs), contributing to syndecan-1 shedding.[10,14,45,46] It is important to mention that the syndecan-1 we detected in the patients' serum could also be a result of other players, such as growth factors and chemokines activated by NS1 or other mechanisms. Additionally, we cannot rule out that syndecan-1 is shed from cells other than endothelial cells.

Due to limited amounts of YF samples available, other valuable analyses such as *in vitro* syndecan-1 shedding by endothelial cells treated with serum samples and endothelial disruption after treatment with YFV NS1-depleted serum samples could not be performed in the present study. Another limitation of this study is that we showed the effects of recombinant YFV NS1 on TEER reduction, syndecan-1 shedding, and sialic acid disruption *in vitro* at concentrations that were higher than the levels of YFV NS1 detected by our ELISA in samples from patients in the severe group. Thus, future studies with additional patient samples will be important to support the hypothesis of the role of NS1 in endothelial disruption during YF disease. It is also important to mention that the samples were collected from individuals seeking hospital treatment, resulting in more severe cases, and that the number of samples were limited. Although sample selection and

size for our study were based on sample availability, it did not depend on exposure factors such as YFV NS1 and syndecan-1 levels or TEER values.

In a previous study by Kallas et al. (2019), older age, male sex, higher leukocyte and neutrophil counts (>4000 cells/mL), AST, bilirubin, creatinine, and viral load (>5.1 log10 copies/mL), as well as prolonged prothrombin time, were associated with increased mortality in patients with YF.[2] Thus, we used these parameters to classify severe cases of YF in our current study, which utilized samples obtained from the same cohort. In a more recent study, hyperimmune activation and perturbation of the gut microbiome related to heightened levels of microbial translocation were also found to be associated with severe outcome in these patients.[47] Moreover, coagulopathy in YF patients from the same cohort and in YFV-infected macaques was not only associated with defects in clotting factor synthesis due to hepatocyte infection, but also with coagulation factor consumption, shown by increased concentrations of plasma D-dimer.[48] Thus, cytokine storm, microbial translocation, and coagulopathy likely contributed to the activation of endothelial dysfunction observed in these patients.

Antigenic cross-reactivity during diagnosis of flaviviral diseases is a major challenge, particularly in endemic settings where multiple flaviviruses co-circulate.[49] Therefore, assays measuring NS1 in sera must be highly specific to avoid incorrect diagnosis. The presence of NS1 is widely used as an early diagnostic marker for flavivirus infections, especially dengue.[50] We produced and tested multiple novel anti-YFV NS1 mAbs when developing our YFV NS1 capture ELISA, aiming for minimal cross-reactivity to other flavivirus NS1 proteins while maintaining the highest sensitivity possible. Because our newly developed YFV NS1 ELISA is highly specific and can detect low concentrations of NS1 in supernatants or sera, it could be used in research and clinical settings, including differential diagnosis of flaviviruses at lower cost compared to molecular assays, with additional potential for prognosis.

Taken together, our study identifies serum levels of YFV NS1 and syndecan-1 as correlates of YF disease severity. Our work suggests that endothelial dysfunction is a major clinical manifestation of human YF, as in dengue, and that circulating NS1 may contribute to this pathogenesis, as has been observed *in vitro* and in murine models. Further, our development of a highly specific YFV NS1 capture ELISA can serve as a proof-of-concept for the development of low-cost NS1-based diagnostics of YF and perhaps be used to predict YF disease progression in humans.

Contributors

FTGS, SBB, ECS, and EH conceived the study; EGK, ECS, and EH acquired funding; FTGS, CMW, ERM, LVT, PHC, LMOP, AN, SB, PRB, and SBB conducted experiments; FTGS and JVZ performed data verification; ERM, LGFABD'EZ, Y-LH, CMR, and EGK conducted the cohort studies; FTGS, CMR, PRB, SBB, EGK, ECS, and EH provided supervision; FTGS and CMW designed figures; FTGS and JVZ performed statistical analysis; FTGS wrote the original draft of this manuscript; FTGS, CMW, CMR, PRB, SBB, and EH edited subsequent drafts. All authors read and approved the final version of the manuscript.

Data sharing statement

Data may be available upon request submitted to corresponding authors E.H or E.C.S. Individual data for reproducing figures may be shared with outside investigators following University of São Paulo and University of California–Berkeley IRB approvals, as data may contain potentially identifying patient information. The materials and data used in this study are covered by standard data and material transfer agreements.

Declaration of interests

The authors declare no conflict of interests.

Acknowledgements

We thank Marcus Wong and Sandra Bos for their assistance in the revision of the manuscript, Amaro Nunes Duarte-Neto for helpful discussions, and Jaime Cardona-Ospina for his feedback on statistical approaches. This study was supported by NIH grants, R01 AI24493 and AI168003 (E.H.), and by São Paulo Research Foundation-FAPESP (Project #2013/01690-0 to ECS and Scholarships #2013/01702-9 and 2017/16627-3 to FTGS). SBB was supported in part as an Open Philanthropy Awardee of the Life Sciences Research Foundation.

Appendix A. Supplementary data

Supplementary data related to this article can be found at https://doi.org/10.1016/j.ebiom.2024.105409.

References

1 Kraemer MU, Faria NR, Reiner RC, et al. Spread of yellow fever virus outbreak in Angola and the Democratic Republic of the Congo 2015–16: a modelling study. *Lancet Infect Dis*. 2017;17:330–338.
2 Kallas EG, D'Elia Zanella LGFAB, Moreira CHV, et al. Predictors of mortality in patients with yellow fever: an observational cohort study. *Lancet Infect Dis*. 2019;19:750–758.
3 Gardner CL, Ryman KD. Yellow fever: a reemerging threat. *Clin Lab Med*. 2010;30:237–260.
4 Glasner DR, Puerta-Guardo H, Beatty PR, Harris E. The good, the bad, and the shocking: the multiple roles of dengue virus nonstructural protein 1 in protection and pathogenesis. *Annu. Rev. Virol*. 2018;5:227–253.
5 Libraty DH, Young PR, Pickering D, et al. High circulating levels of the dengue virus nonstructural protein NS1 early in dengue illness correlate with the development of dengue hemorrhagic fever. *J Infect Dis*. 2002;186:1165–1168.
6 Paranavitane SA, Gomes L, Kamaladasa A, et al. Dengue NS1 antigen as a marker of severe clinical disease. *BMC Infect Dis*. 2014;14:570.
7 Duyen HTL, Ngoc TV, Ha DT, et al. Kinetics of plasma viremia and soluble nonstructural protein 1 concentrations in dengue: differential effects according to serotype and immune status. *J Infect Dis*. 2011;203:1292–1300.
8 Puerta-Guardo H, Glasner DR, Espinosa DA, et al. Flavivirus NS1 triggers tissue-specific vascular endothelial dysfunction reflecting disease tropism. *Cell Rep*. 2019;26:1598–1613.e8.
9 Puerta-Guardo H, Biering SB, de Sousa FTG, et al. Flavivirus NS1 triggers tissue-specific disassembly of intercellular junctions leading to barrier dysfunction and vascular leak in a GSK-3β-dependent manner. *Pathogens*. 2022;11:615.
10 Pan P, Li G, Shen M, et al. DENV NS1 and MMP-9 cooperate to induce vascular leakage by altering endothelial cell adhesion and tight junction. *PLoS Pathog*. 2021;17:e1008603.
11 Wessel AW, Dowd KA, Biering SB, et al. Levels of circulating NS1 impact West Nile virus spread to the brain. *J Virol*. 2021;95:e008444-21.

12 Hui L, Nie Y, Li S, et al. Matrix metalloproteinase 9 facilitates Zika virus invasion of the testis by modulating the integrity of the blood-testis barrier. *PLoS Pathog*. 2020;16:e1008509.
13 Espinosa DA, Beatty PR, Puerta-Guardo H, et al. Increased serum sialic acid is associated with morbidity and mortality in a murine model of dengue disease. *J Gen Virol*. 2019;100:1515–1522.
14 Puerta-Guardo H, Glasner DR, Harris E. Dengue virus NS1 disrupts the endothelial glycocalyx, leading to hyperpermeability. *PLoS Pathog*. 2016;12.
15 Theocharis AD, Skandalis SS, Tzanakakis GN, Karamanos NK. Proteoglycans in health and disease: novel roles for proteoglycans in malignancy and their pharmacological targeting. *FEBS J*. 2010;277:3904–3923.
16 Liu L, Akkoyunlu M. Circulating CD138 enhances disease progression by augmenting autoreactive antibody production in a mouse model of systemic lupus erythematosus. *J Biol Chem*. 2021;297:101053.
17 Manon-Jensen T, Itoh Y, Couchman JR. Proteoglycans in health and disease: the multiple roles of syndecan shedding. *FEBS J*. 2010;277:3876–3889.
18 Suzuki K, Okada H, Sumi K, et al. Serum syndecan-1 reflects organ dysfunction in critically ill patients. *Sci Rep*. 2021;11:1–9.
19 Zhang D, Li L, Chen Y, et al. Syndecan-1, an indicator of endothelial glycocalyx degradation, predicts outcome of patients admitted to an ICU with COVID-19. *Mol Med*. 2021;27:1–12.
20 Suwarto S, Sasmono RT, Sinto R, Ibrahim E, Suryamin M. Association of endothelial glycocalyx and tight and adherens junctions with severity of plasma leakage in dengue infection. *J Infect Dis*. 2017;215:992–999.
21 Mariappan V, Adikari S, Shanmugam L, Easow JM, Pillai AB. Expression dynamics of vascular endothelial markers: endoglin and syndecan-1 in predicting dengue disease outcome. *Transl Res*. 2021;232:121–141.
22 Vuong NL, Lam PK, Ming DKY, et al. Combination of inflammatory and vascular markers in the febrile phase of dengue is associated with more severe outcomes. *Elife*. 2021;10:e67460.
23 McBride A, Duyen HTL, Vuong NL, et al. Endothelial and inflammatory pathophysiology in dengue shock: new insights from a prospective cohort study in Vietnam. *PLoS Neglected Trop Dis*. 2024;18:e0012071.
24 Romano CM, Lauck M, Salvador FS, et al. Inter-and intra-host viral diversity in a large seasonal DENV2 outbreak. *PLoS One*. 2013;8:e70318.
25 Tramontini Gomes de Sousa Cardozo F, Baimukanova G, Lanteri MC, et al. Serum from dengue virus-infected patients with and without plasma leakage differentially affects endothelial cells barrier function in vitro. *PLoS One*. 2017;12:e0178820.
26 Cleveland WS, Grosse E, Shyu WM. Local regression models. In: Chambers JM, Hastie TJ, eds. *Statistical models*. Wadsworth & Brooks/Cole; 1992.
27 Biering SB, Akey DL, Wong MP, et al. Structural basis for antibody inhibition of flavivirus NS1–triggered endothelial dysfunction. *Science*. 2021;371:194–200.
28 Schneider CA, Rasband WS, Eliceiri KW. NIH Image to ImageJ: 25 years of image analysis. *Nat Methods*. 2012;9:671–675.
29 Ritz C, Baty F, Streibig JC, Gerhard D. Dose-response analysis using R. *PLoS One*. 2015;10:e0146021.
30 Conover WJ. *Practical nonparametric statistics*. John Wiley & Sons; 1999.
31 Chambers JM, Freeny A, Heiberger RM. Linear models. In: Chambers JM, Hastie TJ, eds. *Statistical models*. Wadsworth & Brooks/Cole; 1992.
32 Kvålseth TO. Cautionary note about R 2. *Am Stat*. 1985;39:279–285.
33 Gaudette S, Hughes D, Boller M. The endothelial glycocalyx: structure and function in health and critical illness. *J Vet Emerg Crit Care*. 2020;30:117–134.
34 Haynes A III, Ruda F, Oliver J, et al. Syndecan 1 shedding contributes to Pseudomonas aeruginosa sepsis. *Infect Immun*. 2005;73:7914–7921.
35 Joensuu H, Anttonen A, Eriksson M, et al. Soluble syndecan-1 and serum basic fibroblast growth factor are new prognostic factors in lung cancer. *Cancer Res*. 2002;62:5210–5217.
36 Malek-Hosseini Z, Jelodar S, Talei A, Ghaderi A, Doroudchi M. Elevated Syndecan-1 levels in the sera of patients with breast cancer correlate with tumor size. *Breast Cancer*. 2017;24:742–747.
37 Lam PK, McBride A, Le DHT, et al. Visual and biochemical evidence of glycocalyx disruption in human dengue infection, and association with plasma leakage severity. *Front Med*. 2020;7:545813.
38 Buijsers B, Garishah FM, Riswari SF, et al. Increased plasma heparanase activity and endothelial glycocalyx degradation in dengue patients is associated with plasma leakage. *Front Immunol*. 2021;12:759570.
39 Olímpio FA, Falcão LFM, Carvalho MLG, et al. Endothelium activation during severe yellow fever triggers an intense cytokine-mediated inflammatory response in the liver parenchyma. *Pathogens*. 2022;11:1–7.
40 Vasconcelos DB, Falcão LFM, da Ponte LCT, et al. New insights into the mechanism of immune-mediated tissue injury in yellow fever: the role of immunopathological and endothelial alterations in the human lung parenchyma. *Viruses*. 2022;14:2379.
41 Carvalho MLG, Falcão LFM, Lopes JdC, et al. Role of Th17 cytokines in the liver's immune response during fatal yellow fever: triggering cell damage mechanisms. *Cells*. 2022;11:2053.
42 Duarte-Neto AN, Cunha MDP, Marcilio I, et al. Yellow fever and orthotopic liver transplantation: new insights from the autopsy room for an old but re-emerging disease. *Histopathology*. 2019;75:638–648.
43 Giugni FR, Aiello VD, Faria CS, et al. Understanding yellow fever-associated myocardial injury: an autopsy study. *EBioMedicine*. 2023;96:104810.
44 van de Weg CAM, Thomazella MV, Marmorato MP, et al. Levels of angiopoietin 2 are predictive for mortality in patients infected with yellow fever virus. *J Infect Dis*. 2024;230:e60–e64.
45 Puerta-Guardo H, Tabata T, Petitt M, et al. Zika virus nonstructural protein 1 disrupts glycosaminoglycans and causes permeability in developing human placentas. *J Infect Dis*. 2020;221:313–324.
46 Chen H-R, Chao CH, Liu CC, et al. Macrophage migration inhibitory factor is critical for dengue NS1-induced endothelial glycocalyx degradation and hyperpermeability. *PLoS Pathog*. 2018;14:e1007033.
47 Pelletier A-N, et al. Yellow fever disease severity is driven by an acute cytokine storm modulated by an interplay between the human gut microbiome and the metabolome. *medRxiv*. 2021. https://doi.org/10.1101/2021.09.25.21264125v1.
48 Bailey AL, Kang LI, de Assis Barros D'Elia Zanella LGF, et al. Consumptive coagulopathy of severe yellow fever occurs independently of hepatocellular tropism and massive hepatic injury. *Proc Natl Acad Sci USA*. 2020;117:32648–32656.
49 Rathore AP, John AL St. Cross-reactive immunity among flaviviruses. *Front Immunol*. 2020;11:334.
50 Guzman MG, Jaenisch T, Gaczkowski R, et al. Multi-country evaluation of the sensitivity and specificity of two commercially-available NS1 ELISA assays for dengue diagnosis. *PLoS Neglected Trop Dis*. 2010;4:e811.